HHS Public Access

Author manuscript

*J Mol Biol*. Author manuscript; available in PMC 2022 August 20.

Published in final edited form as:

*J Mol Biol*. 2021 August 20; 433(17): 166914. doi:10.1016/j.jmb.2021.166914.

# Structural pharmacology of TRP channels

**Yaxian Zhao**[*], **Bridget M. McVeigh**[*], **Vera Y. Moiseenkova-Bell**

Department of Systems Pharmacology and Translational Therapeutics, Perelman School of Medicine, University of Pennsylvania, Philadelphia, Pennsylvania 19104, USA

## Abstract

Transient receptor potential (TRP) ion channels are a super-family of ion channels that mediate transmembrane cation flux with polymodal activation, ranging from chemical to physical stimuli. Furthermore, due to their ubiquitous expression and role in human diseases, they serve as potential pharmacological targets. Advances in cryo-EM TRP channel structural biology has revealed general, as well as diverse, architectural elements and regulatory sites among TRP channel subfamilies. Here, we review the endogenous and pharmacological ligand-binding sites of TRP channels and their regulatory mechanisms.

## Graphical Abstract

[*]equal contribution

**Yaxian Zhao**: Conceptualization, Visualization, Writing- Original draft preparation, Reviewing and Editing.
**Bridget M. McVeigh**: Conceptualization, Visualization, Writing- Original draft preparation, Reviewing and Editing.
**Vera Y. Moiseenkova-Bell**: Conceptualization, Supervision, Writing - Reviewing and Editing.
**Yaxian Zhao**, **Bridget M. McVeigh**: equal contribution to the manuscript.



Declarations of interest: none

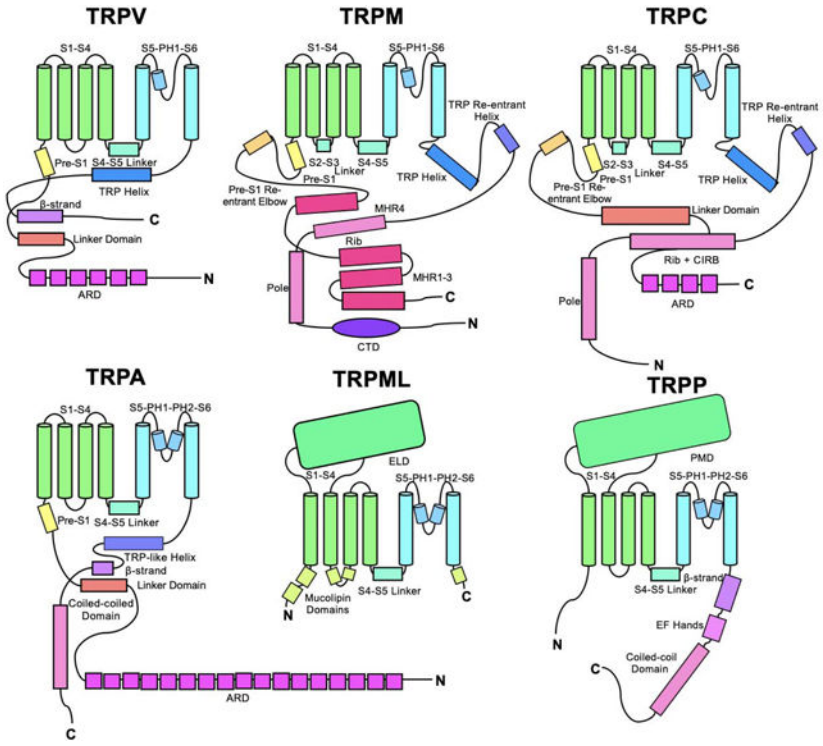


**Keywords**

Ion channels; TRP channel; structural biology; cryo-EM

## Introduction

Mammalian TRP ion channels are a superfamily of non-selective cation permeable, voltage-insensitive ion channels that have diverse physiological and pathophysiological functions and are ubiquitously expressed in different cell types and tissues [1,2]. The first *trp* gene was cloned from *Drosophila melanogaster* retina, where it encodes a phototransduction ion channel that depolarizes the retina in response to light [3]. Since then, 27 members of the mammalian TRP channel superfamily have been identified and divided into six subfamilies based on their sequence homology: TRPV (vanilloid), TRPM (melastatin), TRPC (canonical), TRPA (ankyrin), TRPML (mucolipin), and TRPP (polycystin) [4].

Although a single defining feature of TRP channel function has not yet emerged, they are generally described as polymodal sensors that are responsive to pharmacological ligands, temperature, pH, and mechanical force [1]. Furthermore, TRP channels act as communication centers at the plasma membrane that integrate and amplify diverse signaling pathways [5]. Because of their ubiquitous expression and diversity in regulation and selectivity mechanisms, changes in TRP channel function are associated with a variety of diseases and disease types, such as cardiovascular, respiratory, neurological, and metabolic [6]. Aberrant expression of several TRP channels is also related to cancer development and progression [7]. Their close association with diseases and responsiveness to a variety of

modulators together make TRP channels an attractive target for pharmacological intervention to treat diseases [8].

Recent advances in TRP channel structural biology using cryo-electron microscopy (cryo-EM) have given near-atomic level insights into the molecular basis for their function and pharmacology. To date, at least one structure has been resolved for at least one member of each TRP channel subfamily (Figure 1) [4]. The general architecture of the TRP channel transmembrane domain (TMD) resembles that of voltage-mediated potassium channels ($K_v$): homo- or hetero-tetramers with four subunits surrounding a central ion permeation path. Each subunit has six transmembrane (TM) helices (named S1–S6), with S1–S4 forming the voltage-sensing like domain (VSLD), S5–S6 helices and pore helix (PH) making up the pore domain (PD), and the N- and C-terminus located intracellularly. Adjacent subunits adopt a "domain-swapped" conformation, where the VSLD from one subunit closely interacts with the PD from the adjacent subunit. Like the $K_v$ channel, the ion permeation pathway of TRP channels has two constriction points: the upper ion selectivity filter (SF) lined by the PH and pore loop and the lower gate formed by the C-terminus of S6. In contrast to the conserved arrangement of the TMD, each TRP channel subfamily possesses unique soluble domains that give rise to the diversity in their overall function and architecture across different subfamilies (Figure 1) [9].

Since the boom of cryo-EM, TRP channel structures in complex with small molecules, including agonists, antagonists, and endogenous modulators, have offered insights into TRP channel pharmacological properties. So far, several conserved, as well as channel specific-binding pockets, have been recognized across TRP channel subfamilies. They are found within the TMD or cytoplasmic regions and are frequently located at interfaces between subunits. These small molecules either allosterically regulate the channel gating through coupling mechanisms or directly affecting the conformation of the channel pore [10]. In this review, we first offer a brief overview of TRP channel subfamilies, then describe the major regulatory sites and relevant pharmacological tools that are important for understanding the channel properties, and finally, we discuss and summarize the regulatory mechanisms associated with those modulators. Overall, examining the binding sites of natural and synthetic ligands and the regulatory mechanisms of TRP channels in normal and disease-states will be useful for understanding pharmacological intervention.

## Transient receptor potential (TRP) channel subfamilies

### TRPV (vanilloid) subfamily

The TRPV subfamily has six members that are commonly divided into two groups according to their sequence homology: TRPV1-4 and TRPV5/6. TRPV1-4 are considered thermo-TRPV channels because of their functional role in thermosensation; inflammation, heat, and pain [11]. In contrast, TRPV5/6 are calcium ($Ca^{2+}$)-selective channels that are involved in fine-tuning cytosolic [$Ca^{2+}$] under physiological conditions [12].

Since the first near-atomic resolution TRPV1 structure was resolved in 2013, apo-structures of every member of the TRPV subfamily have been determined, with many in the presence of ligands [13]. A distinguishing feature of the TRPV subfamily is that the N-terminal

ankyrin repeat domain (ARD), composed of six repeats, assembles with the ARDs from other subunits into a characteristic skirt domain that encloses a cytoplasmic cavity. Following the ARDs is a helix-loop-helix (HLH) domain, a linker domain, and a pre-S1 helix that connects to the TMD. After the C-terminus of the S6 helix, the conserved TRP helix runs parallel to the membrane and is sandwiched between the S4–S5 linker and HLH domain. The C-terminal domain (CTD) contains a β-strand that forms an antiparallel β-sheet with two β-strands from the N-terminal linker domain. Together, the pre-S1 helix, HLH domain, linker domain, and the CTD constitute a coupling domain, joining the ARDs to the TMD within the same subunit [14] (Figure 1a).

## TRPM (melastatin) subfamily

The TRPM subfamily has eight members (TRPM1-8) and is the largest and most diverse subfamily of the TRP channel superfamily [15]. It is further subdivided into four groups based on their sequence similarities: TRPM1/3, TRPM4/5, and TRPM/6,7, and TRPM2/8. While most TRPM members are non-selective $Ca^{2+}$-permeable cation channels, TRPM4/5 are only permeable to monovalent cations, like sodium ($Na^{+}$) or potassium ($K^{+}$). Conversely, TRPM6/7 are permeable to magnesium ($Mg^{2+}$) and thus is important in maintaining intracellular $Mg^{2+}$ homeostasis. Unlike other TRP channels, TRPM4/5/8 have been shown to have voltage-dependent gating mechanisms [16]. TRPM channels are known for their involvement in sensing temperature and oxidative stress, controlling cellular death, and taste transduction [16, 17, 18, 19]. Malfunction of TRPM channels is associated with neurodegenerative diseases, cardiovascular dysfunction, metabolic disorders, and inflammatory diseases [20, 21, 22, 23].

A distinguishing feature of TRPM channels is a three-layered assembly: TMD, melastatin homology regions (MHR) 3/4 and MHR 1/2. MHR1/2 have a β-strand core that is surrounded by short α-helices. MHR3/4 are stacks of α-helices that are connected to the TMD via the pre-S1 domain, which has a cytosolic α-helix (pre-S1 shoulder) and an HLH (pre-S1 elbow). After the TRP helix, there is a small membrane embedded TRP re-entrant helix that is connected to the CTD. The CTD of TRPM channels has a unique umbrella shape, with a horizontally positioned rib helix (coiled-coil domain) running parallel to the TRP helix, and a vertical pole helix (coiled-coil domain) that is located underneath the central ion conducting pore. The rib-and pole-helix penetrate the tunnels surrounded by MHR regions and forms a complicated network that transduces and propagates the intracellular signals to the PD. TRPM2/6/7 all have a unique enzymatically active protein domain within their structures. TRPM2 has a C-terminal ADP-ribose (ADPR) pyrophosphatase homology domain (NUDT9-H) located underneath the N-terminal MHR regions. TRPM6/7 have protein kinase activity, with a C-terminal α-type serine/threonine kinase domain. One striking feature of the intracellular domains of TRPM channels is that they form an extensive intra- and inter- subunit interface [16]. These interfaces not only support the tetrameric assembly and trafficking of the channel but also serve as receptor sites for a broad spectrum of modulators [24] (Figure 1b).

### TRPC (canonical) subfamily

TRPC channels are considered the founding member of the TRP superfamily because they are the closest homologues to the *Drosophila melanogaster* TRP channel. The TRPC subfamily is comprised of seven members that are divided into four subgroups based on their primary sequence and activation mechanisms: TRPC3/6/7, TRPC1, TRPC/4/5, and TRPC2, which is a pseudogene in humans. TRPC3/6/7 can be directly activated by diacylglycerol (DAG), which is generated from the cleavage of phosphatidylinositol 3,5-bisphosphate ($PI(3,5)P_2$) by phospholipase C (PLC) via G-protein coupled receptor (GPCR) or receptor tyrosine kinase [25]. Although TRPC1 and TRPC4/5 are generally considered to be DAG-insensitive, a recent study showed that TRPC4 and TRPC5 can become DAG-sensitive upon removal of the attached $Na^+/H^+$ exchanger regulation factor [26, 27]. Additionally, TRPC channels are regulated by several molecules in the PLC pathway, including inositol triphosphate ($IP_3$), $PI(3,5)P_2$, $Ca^{2+}$-calmodulin (CaM), and intracellular $Ca^{2+}$ [28].TRPC channel function is enigmatic, but it's hypothesized to be involved in store- and receptor-operated $Ca^{2+}$ entry. Furthermore, they have been shown to be implicated in kidney, cardiovascular, and neurological diseases. [29].

The intracellular domains of TRPC channels shares similar topology to TRPM channels. The N-terminal domain (NTD) of TRPC channels contains four ARs, a HLH domain, and the re-entrant pre-S1 elbow. The CTD consists of the horizontally positioned rib helix (coiled-coil domain), which runs parallel with the TRP domain, followed by the vertically positioned pole helix (coiled-coil domain) [28]. TRPC channels deviates from the classic TMD arrangement in two ways. First, the S3 helix of TRPC3/6 channels is about three turns longer than that of TRPC4/5 channels. The extralong extracellular protrusion of TRPC3/6 may be important for interacting with extracellular ligands and modulators [29]. Second, two conserved cysteine residues that exist only in TRPC1 and TRPC4/5 form a disulfide bond at the loop connecting the S5 helix and PH. This disulfide bond is involved in stabilizing the pore conformation and sensing the redox environment [30, 31]. Furthermore, a C-terminal CaM and $IP_3$ receptor binding (CIRB) motif is conserved in all TRPC channels, which is essential for regulation [32] (Figure 1c).

### TRPA (ankyrin) subfamily

The TRPA subfamily has a lone member, TRPA1, also known as the wasabi receptor. TRPA1 is mainly expressed in nociceptive neurons and non-neuronal cells, such as epithelial cells. It can be activated by a broad spectrum of noxious stimuli: intense cold, pungent compounds, and environmental irritants. TRPA1 has become an attractive pharmacological target because of its involvement in inflammation and pain for related conditions such as familial episodic pain syndrome, asthma, and cough [33].

Indicative of its name, TRPA1 possesses a long N-terminal tail with an ARD composed of 17 ARs. The arrangement of the NTD is similar to that of TRPV channels, with the large N-terminal ARDs connected to the TMD via a linker domain and pre-S1 domain. The linker domain has a stack of short α-helices and two β-strands, which forms a β-sheet with the β-strand in the CTD. TRPA1 has a classic TMD arrangement except that it has two PH (PH1 and PH2). The CTD has a β-strand connected to the TRP-like helix, a short helix, and a

vertically positioned coiled-coil domain. The linker domain, pre-S1 domain, and TRP-like helix together form a coupling domain that harbors a binding pocket for electrophilic agonists [34, 35] (Figure 1d). Although sequence analysis shows that human (h)TRPA1 has 17 ARs, the currently available cryo-EM structures of TRPA1 only have five proximal ARs (ARD stem) resolved, with the distal ARs forming a crescent shape surrounding the coiled-coil domain under negative stain images[34]. Thus, its hypothesized that the NTD is highly flexible in nature.

## TRPML (mucolipin)subfamily

The TRPML subfamily, formally known as MCOLN, has three family members, TRPML1-3. Overall, TRP channels are predominantly localized to the plasma membrane, but TRPML channels localize to late endosomes and lysosomes and are extensively involved in the endocytotic pathway [36, 37]. Mutations disrupting TRPML1 function cause the lysosomal storage disease mucolipidosis type IV [38, 39, 40].

Structurally, TRPML channels share similar TMD topology to other TRP channels but are distinct as none of them have a large intracellular NTD or CTD and lack commonly seen structural motifs, like ARs and the TRP domain. However, a distinguishing structural hallmark of the TRPML subfamily is a large extracytosolic/luminal domain (ELD) between S1 and S2 that protrudes out of the membrane for sensing environmental $Ca^{2+}$ and proton concentration [41, 42]. The PD of TRPML1 channels contains two PH (PH1 and PH2), as in TRPA1. The intracellular side of the S1–S3 helices are extended from the membrane to form the mucolipin domains and serve as a recognition site for $PI(3,5)P_2$ and $PI(4,5)P_2$ [43] (Figure 1e).

## TRPP (polycystin) subfamily

TRPP channels were first identified due to mutations in TRPP1 (*Pkd2* gene) causing autosomal dominant polycystic kidney disease, a prevalent and potentially lethal monogenic disorder that causes renal, liver, and pancreatic cysts with subsequent loss of renal function [44, 45]. According to sequence homology, TRPP channels are divided into two groups, PKD1 and PKD2. The PKD1 group of proteins (PKD1, PKDREJ, PKD1LD, PKD1L2 and PKD1L3) contain 11 TM helices, a large extracellular domain, and an intracellular CTD. PKD1 proteins do not function independently as ion channels but form a hetero-oligomeric complex with PKD2 channels (3:1) on primary cilia in the renal epithelium [46, 47, 48]. In contrast, the PKD2 (TRPP) group of channels has three members: TRPP1 (TRPP2, PKD2, APKD2), TRPP2 (TRPP3, PKDL2, PKDL, PKD2L), and TRPP3 (TRPP5, PKD2L2). They have similar TMD architecture as seen in other TRP channels [48, 49]. TRPP1 is primarily localized to the endoplasmic reticulum (ER) and plasma membrane, TRPP2 to the ER, and TRPP3 on the plasma membrane and/or ER [50].

The general architecture of TRPP channels is highly analogous to TRPML channels, with a large extracellular polycystin domain (PMD), equivalent to the ELD domain of TRPML, between S1 and S2 helices, and with two PH (PH1 and PH2). Also, like TRPML channels, they do not contain ARs or a TRP domain. A unique feature of TRPP channels is the C-

terminal EF-hand motifs for binding $Ca^{2+}$ and a coiled-coil domain, which is essential for PKD1-PKD2 interaction [51, 52] (Figure 1f).

## Major ligand-binding pockets and their regulatory mechanisms

### Vanilloid-binding pocket

The vanilloid-binding pocket is a conserved ligand binding site shared across several TRP channel subfamilies [10]. It is a cavity in the TMD surrounded by the S3 helix and S4–S5 linker from one subunit and S6 helix from the adjacent subunit. In the absence of exogenous ligands, the vanilloid-binding pocket is occupied by a phosphatidylinositol (PI) lipid in some TRP channels. It is proposed that in the apo-state a PI lipid stabilizes the channel in its closed state, while a vanilloid agonist displaces the PI lipid from the pocket, opening and activating the channel [53].

Although this pocket was previously predicted, it was first seen by Cao et al. in their structures of rat (r) TRPV1 bound to agonists resiniferatoxin (RTX)/ Double-knot toxin (DkTx) (PDB: 3J5Q) or capsaicin (PDB: 3J5R) [54]. Following this, Gao et al. solved rTRPV1 in complex with RTX/DkTx in nanodiscs (PDB: 5IRX) [53]. Both of the vanilloid agonists (RTX and capsaicin) were discovered binding in the vanilloid pocket – a cavity in the TMD surrounded by the S3 helix (Tyr511) S4 helix (Met547 and Thr550) and S4–S5 linker (Glu570 and Arg557) from one subunit and S6 helix from the adjacent subunit [53, 54]. While exposure to capsaicin was unable to trap the channel in an open state, addition of DkTx traps TRPV1 in its fully open state. The $rTRPV1_{RTX/DkTx}$ structure shows that displacement of the resident PI lipid induces opening of the SF and lower gate via downward tilt movement of the PH away from the central axis and movement of the S5 and S6 helices [53, 54]. Displacement of PI and binding of vanilloid agonist RTX to rTRPV1 promotes formation of a salt bridge between Arg557 of S4 helix and Glu570 of S4–S5 linker, which pulls the S4–S5 linker away from the channels central axis and opens the lower gate, while the SF remains unchanged [53, 54]. Additionally, a vanilloid antagonist, capsazepine, is found to bind to the same hydrophobic pocket as RTX in rTRPV1 but doesn't promote formation of the salt bridge between Arg557 of S4 helix and Glu570 of S4–S5 linker (PDB: 5IS0) [53]. Mutational studies of the vanilloid pocket have determined the following residues as critical for vanilloid agonist binding Thr550 and Met547 from the S4 helix and Tyr511 from the S3 helix of one subunit. (Figure 2a) [54, 55]. One notable residue is Tyr511, which adopts different rotamers to accommodate and fit RTX, increasing its affinity [55].

Although TRPV2/3 share a high degree of sequence similarity with TRPV1, they are not responsive to vanilloid agonists. However, they can be converted into vanilloid-sensitive channels by mutating specific residues lining the vanilloid-binding pocket and PD [56, 57]. This finding suggests that the coupling pathway between the vanilloid agonist binding to the channel and subsequent activation remains conserved in TRPV channels.

Other pharmacological modulators that are found in the position analogous to the vanilloid-binding pocket includes TRPV5 antagonist econazole (ECN) (PDB: 6B5V) and TRPC6 antagonist 2-(benzo[d][1,3]dioxol-5-ylamino)thiazol-4-yl)((3S,5R)-3,5-dimethylpiperidin-1-

yl)methanone (BTDM) (PDB: 5YX9) [29, 58]. The rabbit $TRPV5_{ECN}$ structure revealed coordination of ECN to residues in the S3 and S4 helices, S4–S5 linker, and S6 helix of an adjacent subunit. Due to the limited resolution, mutations were necessary to identify this binding pocket. Specifically, Phe425 of S3 helix is essential for ECN inhibition. ECN binding induces constriction of the lower gate via the movement of the S1–S4 bundle and S4–S5 linker away from the pore axis causing a change in the loop between the S6 helix and the TRP domain (Figure 2a) [58]. In the $hTRPC6_{BTDM}$ structure BTMD associates with Trp526 of S3 helix, S4 helix, Trp624 of S4–S5 linker and Ile640 of S5 helix and Thr714 of S6 helix of an adjacent subunit. There are small conformational changes in the VSLD and S5–S6 pore, rotating toward the central axis and inactivating and closing the channel [29].

Recently, hTRPA1 in complex with GNE551, a non-covalent agonist that does not induce channel desensitization (PDB: 6X2J), was determined. GNE551 binds between the S3 helix, S4 helix (Tyr840), and S4–S5 linker of one subunit and the S5 helix (Ser887) and S6 helix (Gln940) of an adjacent subunit. The $hTRPA1_{GNE551}$ structure is in a non-conducting state and there were no observed structural changes. However, this is the first study to show biased agonism of TRPA1 (Figure 2a) [59]. A recent study using structure-based alignment of TRP channels showed that the hydrophobic residues that surround the vanilloid pocket are largely conserved in all TRP channels, suggesting that the pocket is able to accommodate various hydrophobic molecules [10].

### Voltage sensing-like domain (VSLD)-binding pocket

The VSLD-binding pocket is a hydrophobic cavity that is located on the cytosolic side of the S1–S4 bundle, sitting on top of the TRP helix. In the absence of exogenous ligands, the VSLD-binding pocket of TRP channels is commonly found to be occupied by lipids and cation cofactors, such as $Ca^{2+}$.

$Ca^{2+}$ is an essential cofactor that can regulate various conformations of TRP channel gating, activation, inactivation, and desensitization, by either interacting directly with the channel or interfering with $Ca^{2+}$-dependent signaling pathways [60, 61]. Furthermore, numerous endogenous and exogenous modulators regulate TRP channels in a $Ca^{2+}$-dependent way. A highly conserved $Ca^{2+}$-binding site has been identified in the VSLD-binding pocket of TRPM2 (PDB: 6DRJ, 6MJ2, 6CO7, 6D73, 6PUS, 6PUU), TRPM4 (PDB: 6BQV, 5WP6), TRPM8 (PDB: 6NR3, 6NR4, 6BPQ, 6O77), TRPA1 (PDB: 6V9W), TRPC4 (PDB: 5Z96, 6BQV), and TRPC5 (PDB: 6AEI) [30, 31, 62, 63, 64, 65, 66, 67, 68, 69, 70, 71, 72, 73]. Consistent with sequence alignments, the $Ca^{2+}$ is coordinated by Gln, Tyr, Asn, and two Glu of the S2–S3 α-helix, which is not conserved in TRPV, TRPML, or TRPP channels [10, 71]. Functional studies show that mutating the $Ca^{2+}$ coordinating residue(s) results in a loss of $Ca^{2+}$-dependent modulation of TRP channel agonists in TRPC5, TRPM8, and TRPA1 [31, 71, 72]. Although the binding site for $Ca^{2+}$ is well accepted, its regulatory mechanism(s) remain elusive.

In TRPM8, exogenous agonists and antagonists have been captured binding within the VSLD-binding pocket. An analog of menthol, WS-12, and the super cooling agent, icilin, are potent TRPM8 agonists, with icilin activation requiring $Ca^{2+}$. The cryo-EM structure of collared flycatcher (cf) of $TRPM8_{class\ 1}$ in complex with icilin, $Ca^{2+}$, and positive regulator

PI(4,5)$P_2$ (PDB: 6NR3 and 6NR4) and with WS-12 and PIP(4,5)$_2$ (PDB: 6NR2), shows icilin (and WS-12) surrounded by polar residues lining the S1–S4 bundle and TRP helix, with PI(4,5)$P_2$ binds within a cavity formed by the pre-S1, S4 and S5 helices, and TRP helix and MHR4 from an adjacent subunit [70]. The polar residues lining the cooling agent binding pocket in TRPM8 are conserved in TRPM2/4 and less conserved in TRPM7, but are not conserved in TRPV, TRPML, or TRPP channels [10]. Icilin and WS-12 interact with the S1 helix (Tyr745), S4 helix (Arg841), and TRP helix (Tyr1004) (Figure 2b). Compared to the cfTRPM8 apo-structure (PDB: 6BPQ), icilin-$Ca^{2+}$-PI(4,5)$P_2$ binding causes a rigid body rotation of the VSLD away from the PD, subsequently triggering an α- to $3_{10}$-helical transition at the lower half of the S4 helix, and overall, it is hypothesized that the movement of the S6 helix and bending of the PH widens the gate [69, 70].

Complementary to the study above, the cryo-EM structure of *Parus major* TRPM8 in complex with antagonists (AMTB or TC-I 2014) and $Ca^{2+}$-bound states were determined. Like the agonist cooling agents, both AMTB (PDB: 6O6R) and TC-1 2014 (PDB:6O72) are bound within the VSLD-binding pocket, confirming the promiscuity and adaptability of this pocket to bind structurally distinct ligands. In the apo-like antagonist-bound structure, all the TMD helices are straight and α-helical, and the bend at the S4–S5 linker is lacking. However, in comparison, the $Ca^{2+}$-bound structure (6O77), which closely resembles the icilin-$Ca^{2+}$-PIP(4,5)$_2$-bound (PDB: 6NR3 and 6NR4) structure, there is an α- to $3_{10}$-helical transition at the S4 helix, formation of the S4–S5 linker, and a α- to π-helix transition at the PH and S6 helix. This transition shifts the register of the lower gate and reduces the hydrophobic seal. Noticeably, the TRP helix undergoes significant outward tilting in both the icilin-$Ca^{2+}$-PIP(4,5)$_2$-bound (PDB: 6NR3 and 6NR4) and $Ca^{2+}$-bound structures (PDB: 6O77). Therefore, it is proposed that ligand binding in the VSLD-binding pocket either fixes (antagonists) or disrupts (agonist and $Ca^{2+}$) the relative position between the TRP helix and the VSLD bundle thereby changing the conformational state of the pore [70, 73].

In hTRPC6, an antagonist AM-1473 (PDB: 6UZA) is also found in the VSLD-binding pocket, specifically interacting with His446 and Lys442 of S1 helix, Glu509 of S2 helix, Asp530 and Gln527 of S3 helix, Arg609 of S4 helix, Arg758 of the re-entrant loop, and Tyr753 of the TRP helix. The $hTRPC6_{AM-1473}$ structure shares a similar apo-like state to $hTRPC6_{BTDM}$ (PDB: 5YX9) where S1–S4 and S4–S5 linker adopt a slightly upwards conformation compared to the agonist-bound structure (Figure 2b) [74].

The structural adaptability of the VSLD cavity between different TRP channels makes it a potential target for chemical structure-based compound screening and disease-related drug design. Using a fluorometric imaging plate reader assay, TRPC4/5 selective modulators were identified, an antagonist GFB-8438 and GFB-8749 and agonist GFB-9289 [75]. The structure of zebrafish TRPC4 in complex with antagonist GFB-8438 (PDB: 7B0S) and GFB-8749 (PDB: 7B05) and agonist GFB-9289 (PDB: 7B16) show that both chemical compounds are surrounded by positively charged and aromatic residues in the S1–S4 bundle and TRP helix. In comparison to the apo-state of zebrafish TRPC4 (PDB: 7B0J), GFB-8438, GFB-7B05, and GFB-9298 induce minimal conformational changes at the pore region, even though they have opposing effects *in vivo* [74]. In addition, an *in-silico* drug screening identified a rabbit TRPV5 antagonist ZINC17988990, which binds to negatively charged

residues, Asp406 in S2 helix, aromatic residues, Tyr415 in S2–S3 linker, and S4 helix (PDB: 6PBE). In the rabbit $TRPV5_{ZINC17988990}$ structure the S2 and S3 helices move toward the antagonist, accommodating its binding site and locking it in an inhibited state (Figure 2b) [75]. Furthermore, the TRPV6 antagonist 2-APB binds within the VSLD-binding pocket (refer to 2-APB section).

## Binding pockets near the pore region

Double-knot toxin (DkTx) is a bivalent tarantula peptide with two nearly identical inhibitor cysteine knot (ICK) motifs connected by a linker and activates TRPV1 by stabilizing it in the open state. As previously referenced, the structure of rTRPV1 in complex with DkTx/RTX shows two molecules of DkTx residing on top of the outer pore region. Each hydrophobic finger of ICK motifs penetrates the lipid bilayer and inserts into the crevice between the PH and the extracellular side of S6 of an adjacent subunit (PDB: 3J5Q and 5IRX) [53, 54]. The binding of RTX and insertion of DkTx into the pore region induces expansion of the SF, causing Met644 to rotate away from the central axis and wedge into a pocket under the pore loop of an adjacent subunit. Furthermore, Asp646 at the extracellular side of the SF is better positioned to coordinate cations for permeability across the central axis. The $rTRPV1_{RTX/DkTX}$ structure broadens our understanding of the mechanism of toxin regulation in ion channels. In contrast to $Na_v$ and $K_v$ ion channels, the toxin inhibitors block the ion permeation pathway or impede the movement of the voltage-sensing domains in response to change in membrane potential [76]. However, DkTx binding to rTRPV1 promotes opening of the ion permeation pathway and the VSLD remains mostly stationary.

Cannabinoids are natural compounds that are derived from cannabis plant flowers. One that has gained popularity for its therapeutic potential is cannabidiol (CBD), an active ingredient in *Cannabis sativa*. Cannabinoids and their synthetic derivatives have been shown to modulate a broad range of ion channels: $Na_v$, $K_v$, $Ca_v$, TRPV1-4, TRPA1, and TRPM8 [77]. The cryo-EM structure of rTRPV2 with CBD (PDB: 6U88 and 6U8A) showed coordination with hydrophobic and aromatic residues from S6 helix (Leu631) of one subunit and the S5 helix (Leu541), S6 helix, and PH from an adjacent subunit (Figure 2c) [78]. In several other TRP channels, lipids are found to bind in a similar pocket [54, 58, 79, 80, 81, 82]. Although the $rTRPV2_{CBD}$ represents a non-conductive channel, CBD binding induced noticeable changes at the S4–S5 linker and TRP helix, which sheds light on its activating mechanism. A comparison of the apo state (PDB: 6U84 and 6U85) and CBD-bound state (PDB: 6U8A and 6U88) demonstrates that CBD strengthens the coupling between the S4–S5 linker and S5 helix by transforming the loop into a continuous helix, while pulling the S4–S5 linker closer to the S5 helix. The displacement of the S4–S5 linker is accompanied by a rotation and shift of the TRP helix towards the S6 helix, which may ultimately contribute to the expansion of the lower gate [78]. It is worth noting that structure and sequence alignment of TRP channel structures show that the hydrophobic and aromatic residues that form the CBD-binding pocket are highly conserved across many TRP subfamilies and it is likely they are able to bind CBD in this location [10].

The hTRPML1 channel has a binding pocket equivalent to the CBD-binding pocket, which harbors the agonist ML-SA1 (PDB: 6E7Z and 5WJ9) [43, 83]. Similar to the CBD-binding

pocket, the ML-SA1 pocket is lined primarily by hydrophobic and aromatic residues from the S5 (Cys429 and Tyr436) helix, S6 (Phe513) helix, and PH1 (Phe465) of one subunit and the S6 (Tyr499) helix from a neighboring subunit (PDB: 5WJ9) [83] (Figure 2c). However, unlike the $rTRPV2_{CBD}$ complex structure (PDB: 6U88 and 6U8A), where minimal change occurs at the pore region, the $hTRPML1_{ML\text{-}SA1}$ structure demonstrates substantial dilation of the lower gate, showing the open-state [78, 83]. Furthermore, the SF remains constricted, reminiscent of the pore dimension change of the $rTRPV1_{capsaicin}$ structure (PDB: 3J5R) [53]. Upon ML-SA1 binding, the binding pocket facing residues of the S6 (Phe513) helix rotate and pull S6 away from the central axis, resulting in an expansion of the hydrophobic seal of the intracellular gate and a slight widening of the lower part of the SF. Like TRPML1, hTRPML3 undergoes a similar conformational change in the ion conducting pathway upon ML-SA1 binding to the analogous pocket, opening the channel (PDB: 6AYF) [84].

While CBD and ML-SA1 bind to TRP channels in a similar position, the coupling mechanisms that lead to the pore opening may be substantially different. The $rTRPV2_{CBD}$ structure (PDB: 6U88 and 6U8A) shows that CBD can allosterically affect channel gating by triggering movement of the S4–S5 linker and TRP helix, as seen in TRPM channels [78]. In contrast, TRPML channels lack the TRP helix and the effect of ML-SA1 on TRPML1/3 derives directly from the binding and shifting of the S6 and PH (PDB: 5WJ9 and 6AYF) [78, 83, 84].

The cryo-EM structure of hTRPC6 bound to agonist AM-0883 (PDB: 6UZ8) shows binding near the pore and forms hydrophobic interactions with Phe675 and Trp680 of PH of the adjacent subunit and Tyr705, Val706, and Val710 of S6 helix and hydrophilic interactions with Glu672 of PH of the adjacent subunit and Asn702 of S6 helix (Figure 2c) [74]. Through sequence alignment, residues of the PH and S6 engaged AM-0883 binding are conserved across other TRPC members [10]. Although the $hTRPC6_{AM\text{-}0833}$ structure shows minimal conformational changes, the authors suggest that rotation of the S6 helix needed to unwind the hydrophobic seal of the intracellular gate and that this agonist-binding site is occupied by DAG, its native lipid agonist [85].

The hTRPA1 double-antagonist structure (HC030031 and A-967079 (A-96)) (EMD: 6268) first identified the A-96 binding site formed by the S5 and S6 helices and PH1 [34]. Furthermore, Phe909 in PH1 was found to be essential for A-96 inhibition of TRPA1. A recent study of hTRPA1 with antagonist A-96 (PDB: 6V9Y) revealed that it wedges near the S5 helix bend and below PH1, causing an outward flip of Phe877, confirming the previous study. Upon its binding, it prevents the straightening of the S5 helix bend and locks the hTRPA1 structure in its closed apo-like state [71]. As determined by mutagenesis and photocrosslinking, the TRPA1 A-96 binding site also accompanies agonists isoflurane and propofol [86, 87].

### Cytoplasmic domain-binding pocket

Numerous TRP channel modulators have been shown to regulate the channel by interacting with the cytoplasmic domains, which are tightly coupled to the pore region. To date, molecules that are identified bound within the cytoplasmic domains include TRPM4

modulator decavanadate (DVT) and inhibitor adenosine triphosphate (ATP), endogenous TRPM2 agonist ADP-ribose (ADPR), and TRPV3 agonist 2-APB (refer to 2-APB section).

DVT is a highly negatively charged metal molecule that reduces the voltage sensitivity of TRPM4. In the structure of hTRPM4 with DVT (PDB: 5WP6), two DVT densities are observed in the intracellular region of each subunit: the first located at the turning point of the CTD rib (Arg1141) and pole helix (Arg1147) and the second at the interface between MHR1/2 of one subunit and MHR3 of the neighboring subunit [67]. Both DVT sites are surrounded by a high density of positively charged residues (R195, R214, and R421) (Figure 3a). Although TRPM5 has similar sequence homology to TRPM4, it lacks one key residue in DVT1 (Arg1147) and three positively charged arginine residues in DVT2. It is suggested that DVT modulates TRPM4 by gating the CTD and N-terminal MHR [67]. In the $hTRPM4_{ATP}$ structure (PDB: 6BCO and 6BCQ), ATP was found at the interface between MHR domains of two adjacent subunits, overlapping with the second DVT binding site [66]. Upon hTRPM4 binding ATP, the MHR1/2 swings away from the MHR3 of the adjacent subunit and may prevent the concerted movement of the intracellular domains during channel activation, stabilizing the channel in the apo-like closed state [66].

ADPR is a metabolic product that cells release upon oxidative stress and activates TRPM2 in the presence of $Ca^{2+}$. Due to limited resolution, the ADPR-binding sites were not directly observed in the zebrafish TRPM2 (PDB: 6PKX), zebrafish TRPM2 (PDB: 6DRJ), and hTRPM2 (PDB: 6MJ2 and 6MIZ) structures [62, 63, 65]. To reconcile this discrepancy the hTRPM2 structure in the presence of agonist ADPR/$Ca^{2+}$ (PDB: 6PUS) or ADPR (PDB: 6PUR) and antagonist 8-bromo-cyclic ADP-ribose (8-Br-cADPR) (PDB: 6PUU) was solved [73]. In their ADPR-$Ca^{2+}$-bound hTRPM2 structure there were two ADPR densities: one within the MHR1/2 cleft (ADPR1), which bends into a U-shape, and the other within the NUDT9-H domain (ADPR2), which is in an extended shape (Figure 3a). Electrophysiology data shows that both ADPR-binding sites are indispensable for TRPM2 activation, but the antagonist 8-Br-cADPR binds only to the MHR1/2 domain. Together with the fact that the invertebrate sea anemone TRPM2 channel is gated independently of the NUDT9-H domain and zebrafish TRPM2 requires NUDT9-H, it was concluded that MHR1/2 is an evolutionally more conserved ADPR-binding site across TRPM2 orthologues, and the NUDT9-H domain assists ADPR binding in vertebrate TRPM2 [73, 88]. In hTRPM2, ADPR1 is surrounded by Tyr295, the loop between β5 strand and α3 loop, and the two phosphate groups interact with Arg358 and the N-terminus of the α7 helix, and the ribose coordinates with Arg302. ADPR2 is located between Tyr1485 and Asp1431, and the α-phosphate group interacts with Arg1433. Like ADPR1, 8-Br-cADPR adopts a U-shape and interacts with Tyr295 and residues in β5 strand and α3 loop. TRPM2 binding to 8-Br-cADPR does not induce any conformational changes and locks the channel in the apo-like closed state. Comparison of the antagonist- and agonist-bound TRPM2 structures shows that the MHR1/2 goes from open to a bi-lobed closed state via the rotation NUDT9-H domain toward the central axis [73].

### 2-aminoethoxydiphenyl borate (2-APB)-binding pockets

2-aminoethoxydiphenyl borate (2-APB) is a small synthetic compound that can regulate many TRP channels. It serves as an activator in TRPV1-3, TRPA1, and TRPM6 but inhibits TRPV6, TRPM2/7, and TRPC3/6/7 [80, 81]. Although it is not a practical clinical drug, 2-APB is an essential pharmacological tool for studying ion channel properties and structures of TRP channels in complex with 2-APB are of great importance in understanding the mechanisms of receptor-operated gating of different channels.

In 2018, the cryo-EM structures of $hTRPV6_{Tyr467Ala}$ in the presence (PDB: 6D7T) and absence (PDB: 6D7S) of 2-APB were solved [80]. Furthermore, the crystal structure of rTRPV6 (PDB: 6D7O) and $rTRPV6_{Tyr466Ala}$ (PDB: 6D7Q, 6D7P) in complex with or without 2-APB was determined [80]. The hTyr467Ala and rTyr466Ala mutation was generated to increase 2-APB affinity to TRPV6. They found that it bound within a pocket formed between the cytoplasmic opening of the S1–S4 bundle and the membrane-facing side of the TRP helix, analogous to the VSLD-binding pocket in TRPM8 that binds the cooling agent(s). Residues that accommodate 2-APB molecules and potency within the pocket in $rTRPV6_{Tyr466Ala\text{-}2\text{-}APB}$ include Glu402 in S2 helix and Tyr466 and Arg469 in S4 helix (Figure 3b). In comparison to the apo $hTRPV6_{Tyr467Ala}$ open state structure, 2-APB binding pulls the cytoplasmic side of the S3 and S4 helices, and S4–S5 linker toward the TRP helix to accommodate the antagonist and subsequently squeezes out the surrounding activating PI lipids. This rearrangement of the TM helices disturbs the stabilizing hydrogen bonds between the S4–S5 linker and TRP helix, and between the S5 and S6 helices. The closure of the lower gate is accompanied by π- and α-helix transition in the S6 helix, which is proposed to be critical for gating transition in several TRP channels, such as TRPV3 and TRPM8. Additionally, this group determined the structure of rTRPV6 (PDB: 6D7V) and $rTRPV6_{Tyr466Ala}$ (PDB: 6D7X) in complex with brominated 2-APB (2-APB-Br) using X-ray crystallography. To unambiguously define its respective binding site, the heavy bromine atom in 2-APB-Br was used. As determined in the human homologue, the 2-APB binding site is equivalent in the $rTRPV6_{Tyr466Ala\text{-}2\text{-}APB}$ structure [80].

Despite the overall structure similarity among TRPV channels, 2-APB modulates TRPV3 via a separate mechanism and exerts an opposite effect when compared to TRPV6. The TRPV3 2-APB-binding site was identified and is nearly identical in the mouse (m) $TRPV3_{Tyr564Ala}$ (PDB: 6DVZ), $hTRPV3_{Lys169Ala}$ (PDB: 6OT5), and $hTRPV3_{Lys169Ala}$ (PDB: 6UW9) structures [81, 89, 90].

The $mTRPV3_{Tyr564Ala}$ in complex with 2-APB (PDB: 6DVZ) was solved and they found that 2-APB binds in a pocket between the S4–S5 linker domain (His417 and Thr421), the pre-S1 helix (His426 and His430), and the TRP domain (Arg693 and Arg696) (Figure 3b) [89]. The Tyr564Ala mutation was used to increase 2-APB affinity to TRPV3. Besides this 2-APB-binding site, they reported two additional 2-APB sites in their $mTRPV3_{Tyr564Ala}$ structure: one within the VSLD cavity, where it coordinates to Tyr540, Arg487, and Trp483, and the other is at the extracellular side of S1, S2, and S3 helices, where Tyr564 is found. However, these sites need to be further investigated to confirm their importance in 2-APB binding. The $mTRPV3_{Tyr564Ala}$ 2-APB complex is in the open state and 2-APB binding induces downward tilting of the PH, S6 helix to go from an α- to π-helical transition,

shifting it away from the pore. Furthermore, the S6 helices become two helical turns longer and the TRP helices become two helical turns shorter, resulting in the channel to rotate around the PD, pushing the PI lipid out [89].

The structure of $hTRPV3_{Lys169Ala}$ in complex with 2-APB (PDB:6OT5) revealed that 2-APB is located between the pre-S1 domain and TRP helix [90]. The Lys169Ala mutation sensitizes the hTRPV3 channel. The $hTRPV3_{Lys169Ala}$ 2-APB-bound structure has an expanded lower gate, corresponding to the open state. Residues supporting the ligand are either aromatic or positively charged. Binding of 2-APB causes the TRP helix to undergo a swivel, relative to the S6 helix, and the connecting loop between TRP helix and the N-terminus of the S6 helix becomes a continuous helix, suggesting a tightened coupling between TRP helix and the lower gate. The swivel and the formation of the continuous helix are associated with an α- to π-helix transition. Additionally, an increased interaction between the CTD and the components of the NTD (pre-S1, HLH, and the loop of AR 5) was observed in the 2-APB-bound structure. This indicates that the coupling between NTD and CTD are essential for modulating channel activity [90].

The $hTRPV3_{Lys169Ala}$ with (PDB: 6UW9) or without (PDB: 6UW6) 2-APB in nanodiscs was solved. However, in these structures they only found one 2-APB-binding site between the S4–S5 linker, the pre-S1 helix, and the TRP domain [81, 89]. The $hTRPV3_{Lys169Ala}$ 2-APB complex closely resembled the ligand-free open $hTRPV3_{Lys169Ala}$ structure. However, the pore region of $hTRPV3_{Lys169Ala\text{-}2\text{-}APB}$ is in its inactivated state and there is a π- to α-helical transition of the S6 helix, which induces an inward constriction of the central axis. They propose that the PD transition from the open to inactivated state is less tightly coupled to the TRP domain [81].

Recently, rTRPV2 in complex with 2-APB was determined and revealed its binding site between the S5 helix of one subunit and the S4–S5 linker of the adjacent subunit. 2-APB coordinates with His521 and disrupts cation-π interactions between Arg539 of the S4–S5 linker and Tyr525 of the S5 helix of the adjacent subunit (Figure 3b). Although the $rTRPV2_{2\text{-}APB}$ complex is not open, the S4–S5 linker shifts towards the S5 helix and rotates towards the TRP helix, possible indicating a different transitional state of TRPV2 [91].

## Electrophile-binding site

The TRPA1 channel is extremely sensitive to electrophile irritants, which activates the channel by formation of covalent bonds with cysteine residues. Previous mutagenesis studies have identified that a series of cysteine residues located at the N-terminus region are modified during the electrophile-induced activation. Among them is C261, which is the most critical residues conveying the electrophile reactivity to TRPA1 [92, 93, 94].

The first hTRPA1 cryo-EM structure (PDB: 3J9P) revealed the general architecture of the channel and the complicated network composed of the pre-S1 helix and preceding linker domain. Cys621, the widely accepted electrophile reactive residue, was located within the linker domain, but limited resolution impeded visualization of the electrophile [34]. Later, the hTRPA1 structure in the apo-state with a C621S mutation (PDB:6PQQ) and in complex with covalent agonists BITC (PDB: 6PQP) and JT010 (PDB: 6PQO), was solved with

improved resolution. In their structures, the electrophilic agonists are covalently bound to Cys621 [35]. Although the interaction between the electrophilic agonists and TRPA1 are clearly observed, the channel remained closed in the apo-state, while the pre-S1 helix, the linker domain, which has a stack of short helices (H1–H7) and a three stranded beta-sheet (β1.1– β1.3), form a coupling domain for Cys621. The electrophile-binding site is a clamshell-shape pocket, with the H1–H2 loop, which harbors Cys621, forming the bottom half of the clamshell, and the loop between β1.2 and H5 forming the top half (Figure 3c). Upon BITC or JT010 binding, the attachment of ligand molecules to Cys621 induces an upward swing of the activation-loop (top half of the clamshell), activating TRPA1 by acting as a conformation switch [35]. Although BITC and JT010 are structurally different agonists, the local conformational change triggered at the binding pocket remains identical, explaining the ability of TRPA1 to respond to various types of electrophiles. While the electrophilic agonist-bound structures are in the closed state, similar to the apo-state, they propose that the upward swing of the activation loop “switches on” TRPA1 by inducing movement of the pre-S1 helix and a short helix connecting the C-terminal coiled-coil domain and the β-strand (β1.3). The displacement of these two helices could potentially affect the VSLD and PD due to their proximity to the S4–S5 linker [35].

Recently, hTRPA1 in complex with antagonist A-96 (PDB: 6V9Y) and agonists iodoacetamide (IA) (PDB: 6V9X) and its bulky version BODIPY-iodoacetamide (BIA) (PDB: 6V9V) was determined [71]. Similar to the previous finding, IA and BIA covalently modify Cys621 and induce the upward movement of the activation loop. This movement exposes a second reactive site Cys665, which the smaller electrophile IA covalently modifies, while the bulky electrophile BIA stabilizes the activation loop enough and doesn’t require second covalent modification (Figure 3c). Compared to the A-96-bound hTRPA1, the SF of the IA-bound structure is dilated, with Asp951 increasing the outer gates negative electrostatic potential, and the lower gate is slightly widened, indicating an open-state. The conformational change of the pore region is accompanied by the straightening of the S4–S5 linker and S5 helix, and the coordinated upward shift of the PH and S6 helix [71].

## Conclusions

Upon reviewing the interactions between pharmacological and endogenous ligands with their corresponding TRP channel structures, we found a couple of common rules. First, despite TRP channel modulators being chemically and structurally diverse, their binding sites are relatively conserved, even across different TRP channel subfamilies. For instance, the vanilloid-binding pocket not only interacts with several ligands in the TRPV subfamily, but also harbors the TRPC6 antagonist BTMD. Furthermore, in the absence of exogenous ligands, these hydrophobic pockets are commonly occupied by lipids, which stabilize the channel at resting state. Therefore, modulators can regulate TRP channels by competing off the endogenous lipids. Second, although in many of the ligand-bound structures how the signal of the ligand-sensing is transduced to the pore region remains elusive, the interplay between the S4–S5 linker and the TRP helix certainly plays a role in this process. In the resting state, hydrogen bonds and electrostatic interactions have been discovered between these two intimately positioned domains, favoring the closed state. Upon ligand binding, the local conformational change initiates a structural rearrangement that disrupts the stabilizing

interaction between the S4–S5 linker and the TRP helix. The displacement of the S4–S5 linker or TRP helix can then affect the ion permeation pathway diameter by exerting force directly to the PD forming elements, S5 and S6 helices. Intriguingly, the rearrangement between the S4–S5 linker and TRP helix appears to occur regardless of where the ligand binds, such as the distal cytoplasmic domains.

Furthermore, pathogenic gain-of-function mutations in the S4–S5 linker in TRP channels cause constitutively active channels and lack regulation [95]. Although, TRPML and TRPP channels lack the TRP helix, the large luminal domain between S1 and S2 interacts with the TMD and neighboring luminal domain. Therefore, the luminal domain has a similar functional role as the TRP helix, in respect to gating mechanisms, especially since gain-of-function mutations have also been identified in these domains [85, 95, 96]. We conclude that the S4–S5 linker and TRP helix serve as an integral signaling platform that transduces the ligand binding to the ion permeation pathway and their relative position can also be responsible to the fine-tuning of the diverse functional states of the channel.

## References


1. Nilius B, & Owsianik G (2011). The transient receptor potential family of ion channels. Genome Biology. 12 (3), 218. [PubMed: 21401968]
2. Samanta A, Hughes TET, & Moiseenkova-Bell VY (2018). Transient receptor potential (TRP) channels. Subcellular Biochemistry. 87, 141–165. [PubMed: 29464560]
3. Montell C, & Rubin GM (1989). Molecular characterization of the drosophila trp locus: A putative integral membrane protein required for phototransduction. Neuron. 4, 1313–1323.
4. Madej MG, & Ziegler CM (2018). Dawning of a new era in TRP channel structural biology by cryo-electron microscopy. Pflugers Archiv European Journal of Physiology. 470 (2), 213–225. [PubMed: 29344776]
5. Venkatachalam K, & Montell C (2007). TRP channels. Annual Review of Biochemistry. 87 (1), 165–217.
6. Nilius B, Owsianik G, Voets T, & Peters JA (2007). Transient receptor potential cation channels in disease. Physiological Reviews. 87 (1), 165–217. [PubMed: 17237345]
7. Shapovalov G, Ritaine A, Skryma R, & Prevarskaya N (2016). Role of TRP ion channels in cancer and tumorigenesis. Seminars in Immunopathology. 38 (3), 357–369. [PubMed: 26842901]
8. Nilius B, & Szallasi A (2014). Transient receptor potential channels as drug targets: From the science of basic research to the art of medicine. Pharmacological Reviews. 66 (3), 676–814. [PubMed: 24951385]
9. Ramsey IS, Delling M, & Clapham DE (2006). An introduction to TRP channels. Annual Review of Physiology. 68, 619–647.
10. Huffer KE, Aleksandrova AA, Jara-Oseguera A, Forrest LR, & Swartz KJ (2020). Global alignment and assessment of trp channel transmembrane domain structures to explore functional mechanisms. ELife, 9, 58660.
11. Patapoutian A, Peier AM, Story GM, & Viswanath V (2003). Thermotrp channels and beyond: Mechanisms of temperature sensation. Nature Reviews Neuroscience. 4 (7), 529–539. [PubMed: 12838328]
12. van Goor MKC, Hoenderop JGJ, & van der Wijst J (2017). TRP channels in calcium homeostasis: from hormonal control to structure-function relationship of TRPV5 and TRPV6. Biochimica et Biophysica Acta - Molecular Cell Research. 1864 (6), 883–893. [PubMed: 27913205]
13. Liao M, Cao E, Julius D, & Cheng Y (2013). Structure of the TRPV1 ion channel determined by electron cryo-microscopy. Nature. 504 (7478), 107–112. [PubMed: 24305160]
14. Pumroy RA, Fluck EC, Ahmed T, & Moiseenkova-Bell VY (2020). Structural insights into the gating mechanisms of TRPV channels. Cell Calcium. 87, 102168. [PubMed: 32004816]

15. Fleig A, & Penner R (2004). The TRPM ion channel subfamily: Molecular, biophysical and functional features. Trends in Pharmacological Sciences. 25 (12), 633–639. [PubMed: 15530641]
16. Huang Y, Fliegert R, Guse AH, Lü W, & Du J (2020). A structural overview of the ion channels of the TRPM family. Cell Calcium. 85, 102111. [PubMed: 31812825]
17. Simon F, Varela D, & Cabello-Verrugio C (2013). Oxidative stress-modulated TRPM ion channels in cell dysfunction and pathological conditions in humans. Cellular Signalling. 25 (7), 1614–1624. [PubMed: 23602937]
18. McNulty S, & Fonfria E (2005). The role of TRPM channels in cell death. Pflugers Archiv European Journal of Physiology. 451, 235–242 [PubMed: 16025303]
19. Peier AM, Moqrich A, Hergarden AC, Reeve AJ, Andersson DA, Story GM, Earley TJ, Dragoni I, McIntyre P, Bevan S, & Patapoutian A (2002). A TRP channel that senses cold stimuli and menthol. Cell. 108 (5), 705–715. [PubMed: 11893340]
20. Sun Y, Sukumaran P, Schaar A, & Singh BB (2015). TRPM7 and its role in neurodegenerative diseases. Channels. 9 (5), 253–261. [PubMed: 26218331]
21. Abriel H, Syam N, Sottas V, Amarouch MY, & Rougier JS (2012). TRPM4 channels in the cardiovascular system: Physiology, pathophysiology, and pharmacology. Biochemical Pharmacology. 84 (7), 873–881. [PubMed: 22750058]
22. Vennekens R, Mesuere M, & Philippaert K (2018). TRPM5 in the battle against diabetes and obesity. In Acta Physiologica. 222 (2).
23. Romagnani A, Vettore V, Rezzonico-Jost T, Hampe S, Rottoli E, Nadolni W, Perotti M, Meier xM. A., Hermanns C, Geiger S, Wennemuth G, Recordati C, Matsushita M, Muehlich S, Proietti M, Chubanov V, Gudermann T, Grassi F, & Zierler S (2017). TRPM7 kinase activity is essential for T cell colonization and alloreactivity in the gut. Nature Communications. 8 (1), 1917.
24. Gaudet R (2009). Divide and conquer: High resolution structural information on TRP channel fragments. Journal of General Physiology. 133 (3), 231–237.
25. Trebak M, Vazquez G, Bird GSJ, & Putney JW (2003). The TRPC3/6/7 subfamily of cation channels. Cell Calcium. 33 (5–6), 451–461. [PubMed: 12765690]
26. Hofmann T, Obukhov AG, Schaefer M, Harteneck C, Gudermann T, & Schultz G (1999). Direct activation of human TRPC6 and TRPC3 channels by diacylglycerol. Nature. 397, 259–263. [PubMed: 9930701]
27. Storch U, Forst AL, Pardatscher F, Erdogmus S, Philipp M, Gregoritza M, Schnitzler MMY, & Gudermann T (2017). Dynamic NHERF interaction with TRPC4/5 proteins is required for channel gating by diacylglycerol. Proceedings of the National Academy of Sciences of the United States of America, 114 (1), 37–46.
28. Wang H, Cheng X, Tian J, Xiao Y, Tian T, Xu F, Hong X, & Zhu MX (2020). TRPC channels: Structure, function, regulation and recent advances in small molecular probes. Pharmacology and Therapeutics. 209, 107497. [PubMed: 32004513]
29. Tang Q, Guo W, Zheng L, Wu JX, Liu M, Zhou X, Zhang X, & Chen L (2018). Structure of the receptor-activated human TRPC6 and TRPC3 ion channels. Cell Research. 28 (7), 746–755. [PubMed: 29700422]
30. Duan J, Li J, Zeng B, Chen GL, Peng X, Zhang Y, Wang J, Clapham DE, Li Z, & Zhang J (2018). Structure of the mouse TRPC4 ion channel. Nature Communications. 9, 3102.
31. Duan J, Li J, Chen GL, Ge Y, Liu J, Xie K, Peng X, Zhou W, Zhong J, Zhang Y, Xu J, Xue C, Liang B, Zhu L, Liu W, Zhang C, Tian XL, Wang J, Clapham DE, … Zhang J (2019). Cryo-EM structure of TRPC5 at 2.8-Å resolution reveals unique and conserved structural elements essential for channel function. Science Advances. 5 (7), 7935.
32. Vazquez G, Wedel BJ, Aziz O, Trebak M, & Putney JW (2004). The mammalian TRPC cation channels. Biochimica et Biophysica Acta - Molecular Cell Research.1742 (1–3), 21–36.
33. Moran MM (2018). TRP Channels as Potential Drug Targets. In Annual Review of Pharmacology and Toxicology. 58, 309–330.
34. Paulsen CE, Armache JP, Gao Y, Cheng Y, & Julius D (2015). Structure of the TRPA1 ion channel suggests regulatory mechanisms. Nature. 205 (520), 511–517.

35. Suo Y, Wang Z, Zubcevic L, Hsu AL, He Q, Borgnia MJ, Ji RR, & Lee SY (2020). Structural Insights into Electrophile Irritant Sensing by the Human TRPA1 Channel. Neuron. 105 (5), 882–894. [PubMed: 31866091]
36. Venkatachalam K, Wong CO, & Zhu MX (2015). The role of TRPMLs in endolysosomal trafficking and function. Cell Calcium. 58 (1), 48–56. [PubMed: 25465891]
37. Xu H, & Ren D (2015). Lysosomal physiology. Annual Review of Physiology. 77, 57–80.
38. Bargal R, Avidan N, Ben-Asher E, Olender Z, Zeigler M, Frumkin A, Raas-Rothschild A, Glusman G, Lancet D, & Bach G (2000). Identification of the gene causing mucolipidosis type IV. Nature Genetics. 26 (1) 118–123. [PubMed: 10973263]
39. Bassi MT, Manzoni M, Monti E, Pizzo MT, Ballabio A, & Borsani G (2000). Cloning of the gene encoding a novel integral membrane protein, mucolipidin - And identification of the two major founder mutations causing mucolipidosis type IV. American Journal of Human Genetics. 67 (5), 1110–1120. [PubMed: 11013137]
40. Sun M, Goldin E, Stahl S, Falardeau JL, Kennedy JC, Acierno JS, Bove C, Kaneski CR, Nagle J, Bromley MC, Colman M, Schiffmann R, & Slaugenhaupt SA (2000). Mucolipidosis type IV is caused by mutations in a gene encoding a novel transient receptor potential channel. Human Molecular Genetics. 9 (17), 2471–2478. [PubMed: 11030752]
41. Viet KK, Wagner A, Schwickert K, Hellwig N, Brennich M, Bader N, Schirmeister T, Morgner N, Schindelin H, & Hellmich UA (2019). Structure of the Human TRPML2 Ion Channel Extracytosolic/Lumenal Domain. Structure. 27 (8), 1246–1257. [PubMed: 31178222]
42. Li M, Zhang WK, Benvin NM, Zhou X, Su D, Li H, Wang S, Michailidis IE, Tong L, Li X, & Yang J (2017). Structural basis of dual Ca 2+ /pH regulation of the endolysosomal TRPML1 channel. Nature Structural and Molecular Biology. 9 (1), 4192.
43. Fine M, Schmiege P, & Li X (2018). Structural basis for PtdInsP2-mediated human TRPML1 regulation. Nature Communications. 9, 4192.
44. Gabow PA, Chapman AB, Johnson AM, Tangel TJ, Duley IT, Kaehny WD, Manco-Johnson M, & Schrier RW (1990). Renal structure and hypertension in autosomal dominant polycystic kidney disease. Kidney International. 38 (6), 1177–1180. [PubMed: 2074659]
45. Igarashi P, & Somlo S (2002). Genetics and pathogenesis of polycystic kidney disease. In Journal of the American Society of Nephrology. 13 (9), 2384–2398. [PubMed: 12191984]
46. Hanaoka K, Qian F, Boletta A, Bhunia AK, Piontek K, Tsiokas L, Sukhatme VP, Guggino WB, & Germino GG (2000). Co-assembly of polycystin-1 and −2 produces unique cation-permeable currents. Nature. 408 (6815), 990–994. [PubMed: 11140688]
47. Yu Y, Ulbrich MH, Li MH, Buraei Z, Chen XZ, Ong ACM, Tong L, Isacoff EY, & Yang J (2009). Structural and molecular basis of the assembly of the TRPP2/PKD1 complex. Proceedings of the National Academy of Sciences of the United States of America. 106 (28), 11558–11563. [PubMed: 19556541]
48. Su Q, Hu F, Ge X, Lei J, Yu S, Wang T, Zhou Q, Mei C, & Shi Y (2018). Structure of the human PKD1-PKD2 complex. Science. 361 (6406), 9819.
49. Shen PS, Yang X, DeCaen PG, Liu X, Bulkley D, Clapham DE, & Cao E (2016). The Structure of the Polycystic Kidney Disease Channel PKD2 in Lipid Nanodiscs. Cell. 167 (3), 763–773. [PubMed: 27768895]
50. Katsianou MA, Skondra FG, Gargalionis AN, Piperi C, & Basdra EK (2018). The role of transient receptor potential polycystin channels in bone diseases. Annals of Translational Medicine. 6 (12), 246. [PubMed: 30069448]
51. Qian F, Germino FJ, Cai Y, Zhang X, Somlo S, & Germino GG (1997). PKD1 interacts with PKD2 through a probable coiled-coil domain. Nature Genetics. 16 (2), 179–183. [PubMed: 9171830]
52. Tsiokas L, Kim E, Arnould T, Sukhatme VP, & Walz G (1997). Homo- and heterodimeric interactions between the gene products of PKD1 and PKD2. Proceedings of the National Academy of Sciences of the United States of America. 94 (13), 6965–6970. [PubMed: 9192675]
53. Cao E, Liao M, Cheng Y, & Julius D (2013). TRPV1 structures in distinct conformations reveal activation mechanisms. Nature. 504 (7478), 113–118. [PubMed: 24305161]
54. Gao Y, Cao E, Julius D, & Cheng Y (2016). TRPV1 structures in nanodiscs reveal mechanisms of ligand and lipid action. Nature. 534 (7607), 347–351. [PubMed: 27281200]

55. Chou MZ, Mtui T, Gao YD, Kohler M, & Middleton RE (2004). Resiniferatoxin Binds to the Capsaicin Receptor (TRPV1) near the Extracellular Side of the S4 Transmembrane Domain. Biochemistry. 43 (9), 2501–2511. [PubMed: 14992587]
56. Zhang F, Hanson SM, Jara-Oseguera A, Krepkiy D, Bae C, Pearce LV, Blumberg PM, Newstead S, & Swartz KJ (2016). Engineering vanilloid-sensitivity into the rat TRPV2 channel. ELife. 5, 16409.
57. Zhang F, Swartz KJ, & Jara-Oseguera A (2019). Conserved allosteric pathways for activation of TRPV3 revealed through engineering vanilloid-sensitivity. ELife. 8, 42756.
58. Hughes TET, Lodowski DT, Huynh KW, Yazici A, Del Rosario J, Kapoor A, Basak S, Samanta A, Han X, Chakrapani S, Zhou ZH, Filizola M, Rohacs T,Han S, & Moiseenkova-Bell VY (2018). Structural basis of TRPV5 channel inhibition by econazole revealed by cryo-EM. Nature Structural and Molecular Biology. 25 (1), 53–60.
59. Liu C, Reese R, Vu S, Rougé L, Shields SD, Kakiuchi-Kiyota S, Chen H, Johnson K, Shi YP, Chernov-Rogan T, Greiner DMZ, Kohli PB, Hackos D, Brillantes B, Tam C, Li T, Wang J, Safina B, Magnuson S, … Chen J (2020). A Non-covalent Ligand Reveals Biased Agonism of the TRPA1 Ion Channel. Neuron.
60. McGoldrick LL, Singh AK, Saotome K, Yelshanskaya MV, Twomey EC, Grassucci RA, & Sobolevsky AI (2018). Opening of the human epithelial calcium channel TRPV6. Nature. 553 (7687), 233–237. [PubMed: 29258289]
61. Hasan R, & Zhang X (2018). Ca2+ regulation of TRP ion channels. In International Journal of Molecular Sciences. 19 (4), 1256.
62. Huang Y, Winkler PA, Sun W, Lü W, & Du J (2018). Architecture of the TRPM2 channel and its activation mechanism by ADP-ribose and calcium. Nature. 562 (7725), 145–149. [PubMed: 30250252]
63. Wang L, Fu TM, Zhou Y, Xia S, Greka A, & Wu H (2018). Structures and gating mechanism of human TRPM2. Science. 362 (6421), 4809.
64. Zhang Z, Tóth B, Szollosi A, Chen J, & Csanády L (2018). Structure of a TRPM2 channel in complex with Ca2+ explains unique gating regulation. ELife. 7, 36409.
65. Yin Y, Wu M, Hsu AL, Borschel WF, Borgnia MJ, Lander GC, & Lee SY (2019). Visualizing structural transitions of ligand-dependent gating of the TRPM2 channel. Nature Communications. 10 (1), 3740.
66. Guo J, She J, Zeng W, Chen Q, Bai XC, & Jiang Y (2017). Structures of the calcium-activated, non-selective cation channel TRPM4. Nature. 552 (7684), 205–209. [PubMed: 29211714]
67. Winkler PA, Huang Y, Sun W, Du J, & Lü W (2017). Electron cryo-microscopy structure of a human TRPM4 channel. Nature. 552 (7684), 200–204. [PubMed: 29211723]
68. Autzen HE, Myasnikov AG, Campbell MG, Asarnow D, Julius D, & Cheng Y (2018). Structure of the human TRPM4 ion channel in a lipid nanodisc. Science. 359 (6372), 228–232. [PubMed: 29217581]
69. Yin Y, Wu M, Zubcevic L, Borschel WF, Lander GC, & Lee SY (2018). Structure of the cold- And menthol-sensing ion channel TRPM8. Science. 359 (6372), 237–241. [PubMed: 29217583]
70. Yin Y, Le SC, Hsu AL, Borgnia MJ, Yang H, & Lee SY (2019). Structural basis of cooling agent and lipid sensing by the cold-activated TRPM8 channel. Science. 363 (6430), 9334.
71. Zhao J, Lin King JV, Paulsen CE, Cheng Y, & Julius D (2020). Irritant-evoked activation and calcium modulation of the TRPA1 receptor. Nature. 585 (7823), 141–145. [PubMed: 32641835]
72. Diver MM, Cheng Y, & Julius D (2019). Structural insights into TRPM8 inhibition and desensitization. Science. 365 (6460), 1434–1440. [PubMed: 31488702]
73. Huang Y, Roth B, Lü W, & Du J (2019). Ligand recognition and gating mechanism through three Ligand-binding sites of human TRPM2 channel. ELife. 8, 50175.
74. Vinayagam D, Quentin D, Sitsel O, Merino F, Sabrin M, Hofnagel O, Yu M, Ledeboer MW, Malojcic G, & Raunser S (2020) Structural basis of TRPC4 regulation by calmodulin and pharmacological agents. Elife. 9, 60603.
75. Hughes TET, Rosario JS Del, Kapoor A, Yazici AT, Yudin Y, Fluck EC, Filizola M, Rohacs T, & Moiseenkova-Bell VY (2019). Structure-based characterization of novel TRPV5 inhibitors. ELife. 8, 49572.

76. Gilchrist J, Olivera BM, & Bosmans F (2014). Animal toxins influence voltage-gated sodium channel function. Handbook of experimental pharmacology. 221, 203–229. [PubMed: 24737238]
77. Watkins AR (2019). Cannabinoid interactions with ion channels and receptors. Channels (Austin, Tex.) 13 (1), 162–167.
78. Pumroy RA, Samanta A, Liu Y, Hughes TET, Zhao S, Yudin Y, Rohacs T, Han S, & Moiseenkova-Bell VY (2019). Molecular mechanism of TRPV2 channel modulation by cannabidiol. ELife. 8, 48792.
79. Zubcevic L, Herzik MA, Chung BC, Liu Z, Lander GC, & Lee SY (2016). Cryo-electron microscopy structure of the TRPV2 ion channel. Nature Structural and Molecular Biology. 23 (2), 180–186.
80. Singh AK, Saotome K, McGoldrick LL, & Sobolevsky AI (2018). Structural bases of TRP channel TRPV6 allosteric modulation by 2-APB. Nature Communications. 9, 2465.
81. Deng Z, Maksaev G, Rau M, Xie Z, Hu H, Fitzpatrick JAJ, & Yuan P (2020). Gating of human TRPV3 in a lipid bilayer. Nature Structural and Molecular Biology. 27, 635–644.
82. Shimada H, Kusakizako T, Dung Nguyen TH, Nishizawa T, Hino T, Tominaga M, & Nureki O (2020). The structure of lipid nanodisc-reconstituted TRPV3 reveals the gating mechanism. Nature Structural and Molecular Biology. 27, 645–652.
83. Schmiege P, Fine M, Blobel G, & Li X (2017). Human TRPML1 channel structures in open and closed conformations. Nature. 550 (7676), 366–370. [PubMed: 29019983]
84. Zhou X, Li M, Su D, Jia Q, Li H, Li X, & Yang J (2017). Cryo-EM structures of the human endolysosomal TRPML3 channel in three distinct states. Nature Structural and Molecular Biology. 24 (12), 1146–1154.
85. Bai Y, Yu X, Chen H, Horne D, White R, Wu X, Lee P, Gu Y, Ghimire-Rijal S, Lin DCH, & Huang X (2020). Structural basis for pharmacological modulation of the TRPC6 channel. ELife. 9, 53311.
86. Ton HT, Phan TX, Abramyan AM, Shi L, & Ahern GP (2017). Identification of a putative binding site critical for general anesthetic activation of TRPA1. Proceedings of the National Academy of Sciences of the United States of America. 114 (14), 3762–3767. [PubMed: 28320952]
87. Woll KA, Skinner KA, Gianti E, Bhanu NV, Garcia BA, Carnevale V, … Gaudet R (2017). Sites Contributing to TRPA1 Activation by the Anesthetic Propofol Identified by Photoaffinity Labeling. Biophysical Journal. 113 (10), 2168–2172. [PubMed: 28935134]
88. Kühn FJP, Kühn C, & Lückhoff A (2015). Functional characterisation of a TRPM2 orthologue from the sea anemone Nematostella vectensis in human cells. Scientific Reports. 11 (6), 0158060.
89. Singh AK, McGoldrick LL, & Sobolevsky AI (2018). Structure and gating mechanism of the transient receptor potential channel TRPV3. Nature Structural and Molecular Biology. 25, 805–813.
90. Zubcevic L, Borschel WF, Hsu AL, Borgnia MJ, & Lee SY (2019). Regulatory switch at the cytoplasmic interface controls trpv channel gating. ELife. 8, 7746.
91. Protopopova AD, Pumroy RA, de la Roche J, Haugh FM, Sousa BB, Gallo PN, Bernardes GJL, Leffler A, & Moiseenkova-Bell VY (2020). TRPV2 interaction with small molecules and lipids revealed by cryo-EM. bioRxiv.[Preprint]
92. Hinman A, Chuang HH, Bautista DM, & Julius D (2006). TRP channel activation by reversible covalent modification. Proceedings of the National Academy of Sciences of the United States of America. 103 (51), 19564–19568. [PubMed: 17164327]
93. Macpherson LJ, Dubin AE, Evans MJ, Marr F, Schultz PG, Cravatt BF, & Patapoutian A (2007). Noxious compounds activate TRPA1 ion channels through covalent modification of cysteines. Nature. 445 (7127), 541–545. [PubMed: 17237762]
94. Brewster MS, Gaudet R (2015). How the TRPA1 receptor transmits painful stimuli: Inner workings revealed by electron cryomicroscopy. Bioessays. 37 (11), 1184–1192. [PubMed: 26387779]
95. Hofmann L, Wang H, Zheng W, Philipp SE, Hidalgo P, Cavalié A, Chen XZ, Beck A, & Flockerzi V (2017). The S4–S5 linker – gearbox of TRP channel gating.Cell Calcium. 67, 156–165. [PubMed: 28416203]
96. Grieben M, Pike ACW, Shintre CA, Venturi E, El-Ajouz S, Tessitore A, Shrestha L, Mukhopadhyay S, Mahajan P, Chalk R, Burgess-Brown NA, Sitsapesan R, Huiskonen JT, &

Carpenter EP (2017). Structure of the polycystic kidney disease TRP channel Polycystin-2 (PC2). Nature Structural and Molecular Biology. 24, 114–122.

### Current and future perspectives

1. Recent advances in cryo-EM enriched our understanding of the pharmacological and biophysical properties of the polymodal TRP channels.
2. Currently available structures only provide snapshots of TRP channels, which are highly dynamic. Most TRP channel activators do not stabilize the channel in the open state.
3. The essential coupling mechanisms between activator recognition and gating transitions remains mostly unknown. However, we propose that the S4–S5 linker and TRP helix play an important role in transducing the signal.
4. More intermediate transitional states, pre-open, desensitized, or inactivated, and open-state structures are necessary to further elucidate the regulatory mechanisms of activators.
5. Future drug screens could lead to discovery of new (or old) pharmacological tools that could trap TRP channels in different states.

## Highlights

- TRP channel subfamilies have distinguishing structural features
- Conserved binding pockets across TRP channels
- The S4–S5 linker and TRP helix serve as a signaling platform

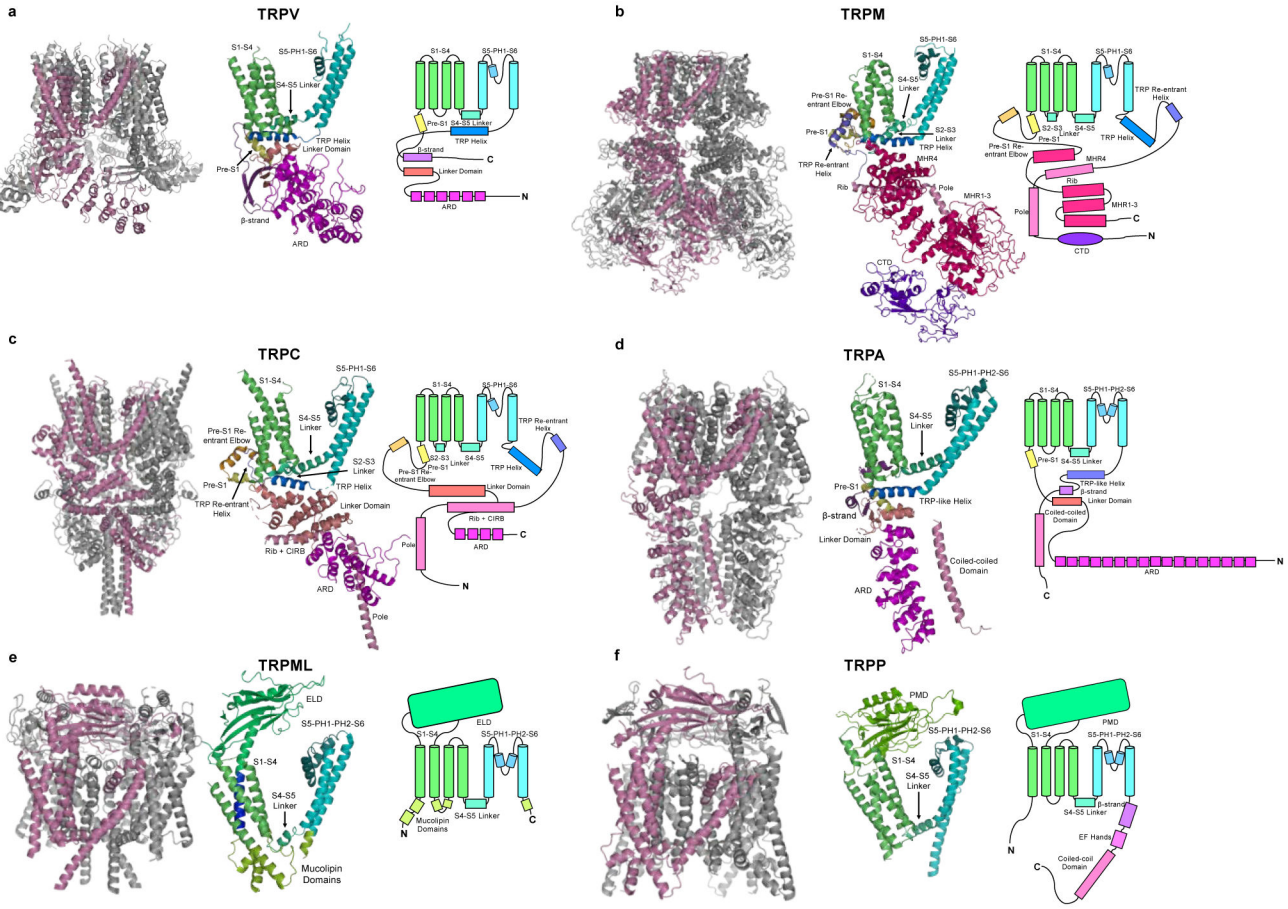


**Figure 1. Representative 3- dimensional organization and architecture of TRP channel subfamilies.**

Single subunit in the 3-dimensional structure is colored pink. The monomer and cartoon representations domains are colored the same. Representative (a) TRPV channel (rTRPV2 PDB: 6U84). Ankyrin repeat domains (ARD) in magenta, linker domain in salmon, pre-S1 helix in pale yellow, S1–S4 helices in lime, S4–S5 linker in green cyan, S5 and S6 helices in cyan, pore helices (PH) in slate, TRP helix in marine, and β-strand in violet. (b) TRPM (hTRPM2 PDB: 6MIX). Melastatin homology regions (MHR) 1–4 in hot pink, pre-S1 re-entrant elbow in orange, S2–S3 linker in green cyan, TRP re-entrant helix in purple blue, rib and pole helices in pink, and C-terminal domain (CTD) in purple. The CTD in TRPM2 has ADP-ribose (ADPR) pyrophosphatase homology domain (NUDT9-H) and TRPM6/7 has an α-type serine/threonine kinase domain. (c)TRPC (TRPC6 PDB: 5YX9). Rib and CRIB domain in pink. (d)TRPA (TRPA1 PDB: 6PQQ). Coiled-coiled domain in pink and TRP-like helix in purple blue. (e)TRPML (TRPML1 PDB: 5WPV). Mucolipin domains in pale green and extracytosolic/luminal domain (ELD) in green. (f) TRPP (TRPP1 PDB: 5K47). Polycystin domain (PMD) in green and EF hands in light magenta.

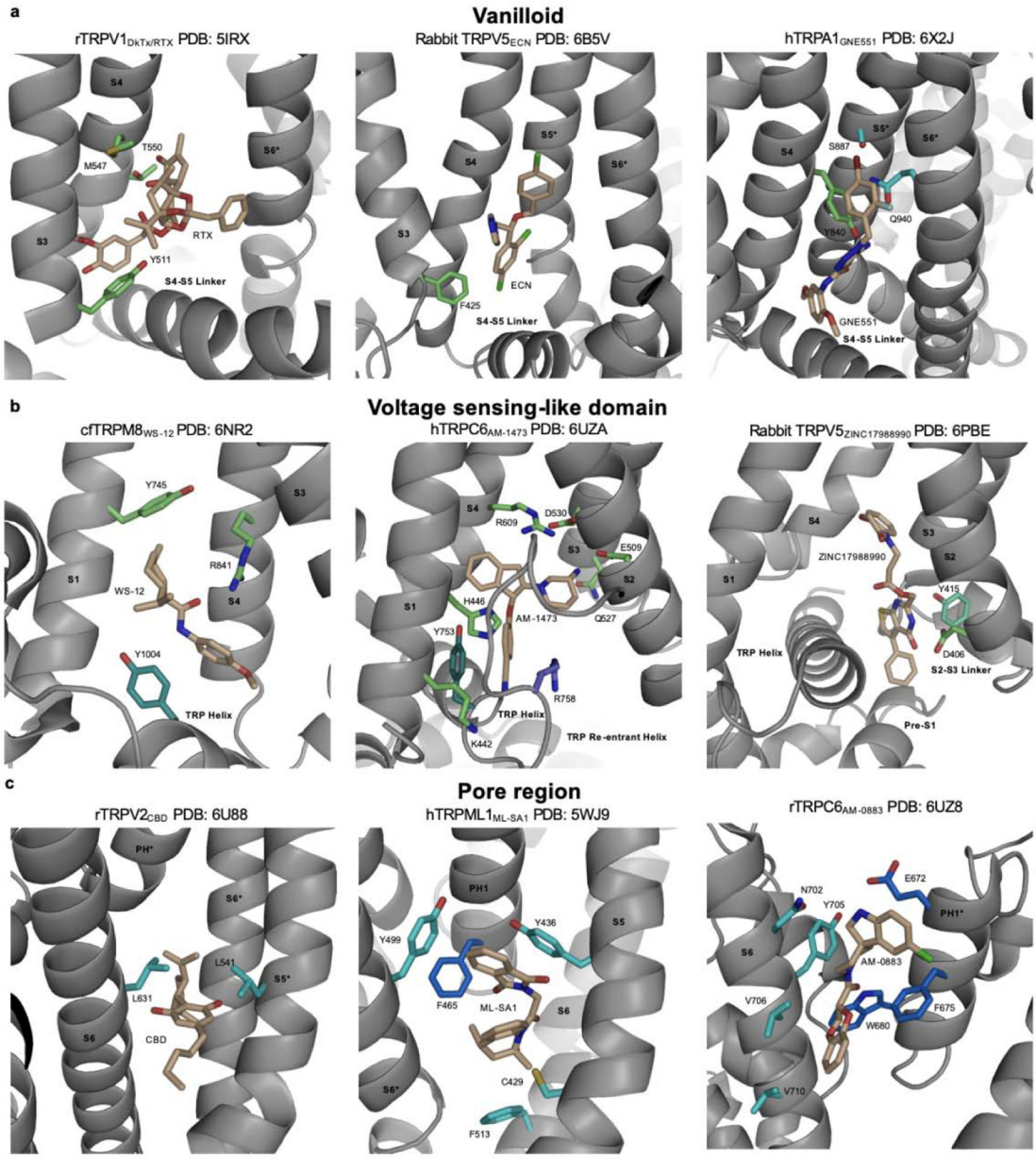


**Figure 2. Model representations of ligand binding sites in (a) vanilloid-, (b) voltage sensing-like domain-, and (c) pore region- binding pockets.**

Ligands are shown as tan sticks Relevant residues targeted in previous mutational studies and conserved residues are shown and are colored to their corresponding sites, labeled, and represented as sticks. Oxygen is shown in red, nitrogen in blue, sulfur in yellow, fluorine in light blue, bromine in dark red, and chloride in green.

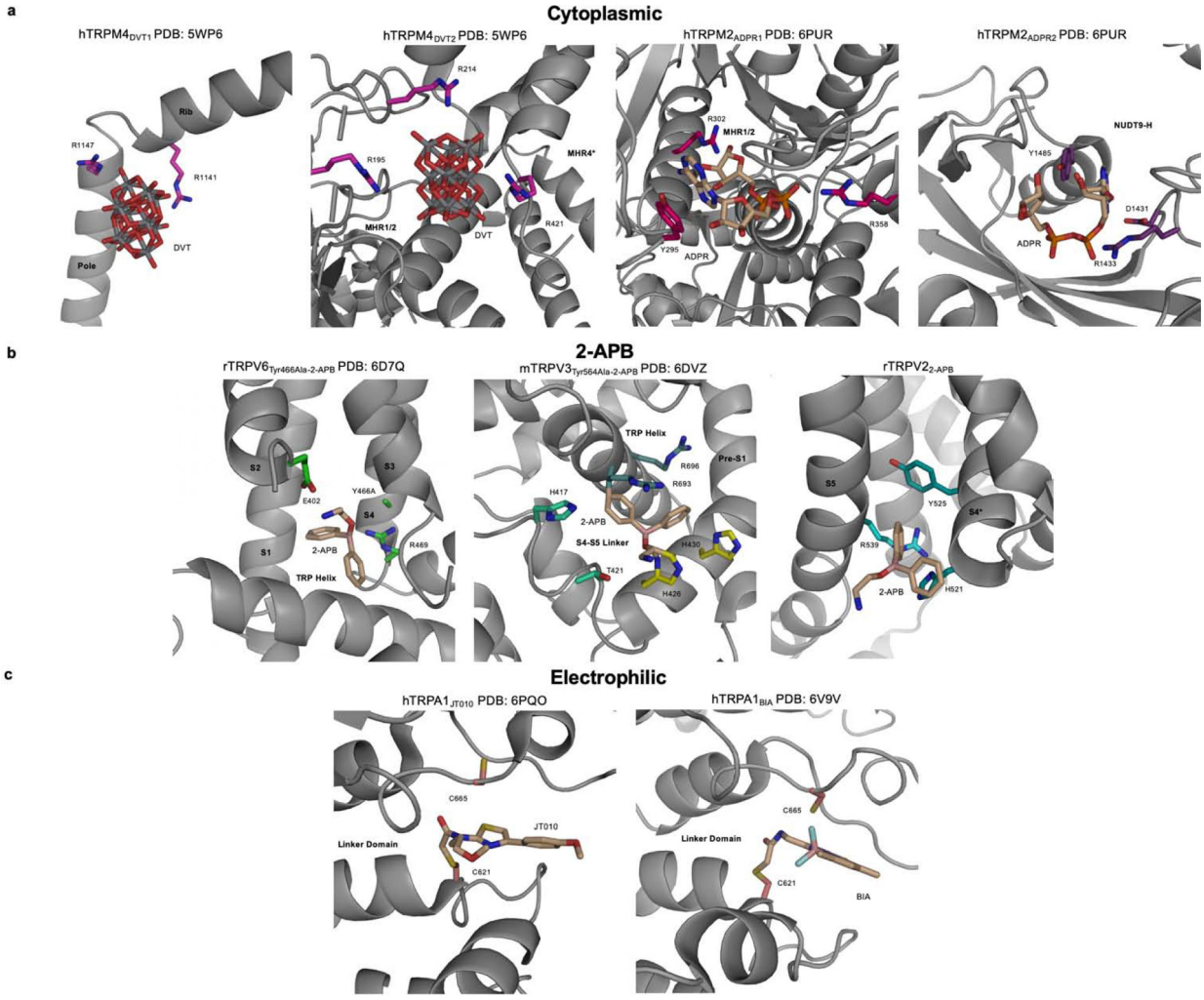


**Figure 3. Model representations ligand binding sites in (a) cytoplasmic-, (b) 2-APB, and (c) electrophile- binding pockets.**

Ligands are shown as tan sticks Relevant residues targeted in previous mutational studies and conserved residues are shown and are colored to their corresponding regions, labeled, and represented as sticks. Oxygen is shown in red, nitrogen in blue, sulfur in yellow, phosphate in orange, fluorine in light blue, boron in pink, and vanadium in grey.